



Contents lists available at ScienceDirect

Spectrochimica Acta Part B

journal homepage: www.elsevier.com/locate/sab

A new spectrometer for grazing incidence X-ray fluorescence for the characterization of Arsenic implants and Hf based high-k layers [☆]

D. Ingerle ^a, F. Meirer ^{a,b}, N. Zoeger ^a, G. Pepponi ^c, D. Giubertoni ^c, G. Steinhauser ^a, P. Wobrauschek ^a, C. Strelia ^{a,*}

^a Atominstytut, Vienna University of Technology, Stadionallee 2, A-1020 Vienna, Austria

^b Stanford Synchrotron Radiation Lightsource, SLAC National Accelerator Laboratory, 2575 Sand Hill Road, Menlo Park CA 94025, USA

^c Fondazione Bruno Kessler, Via Sommarive 18, I-38050 Povo, Italy

ARTICLE INFO

Article history:

Received 15 October 2009

Accepted 15 February 2010

Available online 21 February 2010

Keywords:

GIXRF

Depth profiling

Thin layer characterization

Silicon wafer surface analysis

ABSTRACT

Grazing Incidence X-ray Fluorescence Analysis (GIXRF) is a powerful technique for depth-profiling and characterization of thin layers in depths up to a few hundred nanometers. By measurement of fluorescence signals at various incidence angles Grazing Incidence X-ray Fluorescence Analysis provides information on depth distribution and total dose of the elements in the layers. The technique is very sensitive even in depths of a few nanometers. As Grazing Incidence X-ray Fluorescence Analysis does not provide unambiguous depth profile information and needs a realistic input depth profile for fitting, in the context of the EC funded European Integrated Activity of Excellence and Networking for Nano and Micro-Electronics Analysis (ANNA) Grazing Incidence X-ray Fluorescence Analysis is used as a complementary technique to Secondary Ion Mass Spectrometry (SIMS) for the characterization of Ultra Shallow Junctions (USJ).

A measuring chamber was designed, constructed and tested to meet the requirements of Grazing Incidence X-ray Fluorescence Analysis. A measurement protocol was developed and tested. Some results for As implants as well as Hf based high k layers on Silicon are shown. For the determination of the bulk As content of the wafers, Instrumental Neutron Activation Analysis has also been applied for comparison.

© 2010 Elsevier B.V. All rights reserved.

1. Introduction

In X-ray fluorescence analysis (XRF) the intensity of the wave field is generally assumed to be locally constant *in vacuo* and to be exponentially decreasing in solids. However, in grazing incidence XRF (GIXRF) the primary beam appears as an evanescent wave field or as a standing wave field with locally dependent electric field fluctuations. The intensity of the fluorescence radiation emitted by atoms which are excited by these fields is direct proportional to the wave field intensity. Therefore the fluorescent signal emitted by a sample refers to the varying field intensity of the standing or evanescent wave field within the sample. Moreover it additionally provides information on the elemental composition of the sample. As the distribution of nodes and antinodes of the standing wave field within the sample is a function of the incident angle of the primary radiation the (consequently angle dependent) fluorescence signal can be used for nondestructive depth profiling of layered structures.

For the analysis of thin-film-like samples (“nanofilms”) on a reflecting substrate the analyte has to be positioned within the standing wave

field in front of the substrate. Generally two cases have to be considered for thin films: non-reflecting layers and reflecting layers on the surface of the substrate.

Considering the first case it is assumed that non-reflecting layers should not disturb the primary wave field in front of the substrate significantly. Total reflection of the primary beam does not happen at the nanofilm itself but only at the substrate. The sample is excited to fluorescence and the emitted intensity is proportional to the primary field intensity. The intensity of this field with nodes and antinodes can be calculated with [1]:

$$I(\alpha, z) = I_0 \left[1 + R(\alpha) + 2\sqrt{R(\alpha)} \cos(2\pi z/a - \phi(\alpha)) \right] \quad (1)$$

where I_0 is the intensity of the primary beam, which is assumed to be constant, hitting the surface of the substrate under an angle α . R is the reflectivity of the substrate, z is the height above the surface of the substrate and the argument of the cosine represents the phase difference of the incoming and reflected waves (the travel distance $2\pi z/a$ and a phase shift Φ). This phase shift occurs only in the region of total reflection ($\Phi = 0$ for $\alpha > \alpha_{\text{crit}}$) and is given by:

$$\phi(z) = \arccos\left(2(\alpha/\alpha_{\text{crit}})^2 - 1\right) \quad (2)$$

[☆] This paper was presented at the 13th Conference on Total reflection X-ray Fluorescence Analysis and Related Methods (TXRF 2009), held in Gothenborg, Sweden, 15–19 June 2009, and is published in the Special Issue of Spectrochimica Acta Part B, dedicated to that conference.

* Corresponding author. Tel.: +43 1 58801 14130.

E-mail address: strelia@ati.ac.at (C. Strelia).

Considering a thin film of thickness t the totally emitted intensity of the sample is obtained by integrating Eq. (1) from $z=0$ to $z=t$. In the angular region of total reflection strong oscillations occur for thicknesses smaller than about 100 nm because only a few nodes and antinodes of the standing wave field penetrate the nanofilm.

In the next paragraph reflecting layers are discussed. They are assumed to be flat, smooth and of constant thickness (about 0.2–100 nm) over the entire surface of the substrate. The angle dependent fluorescence emitted by such layers excited by X-rays can be calculated by means of fundamental parameters. First the primary intensity within the layer has to be computed as a function of penetration depth. Then excitation to fluorescence, absorption and enhancement must be included in the calculation. Eventually the fluorescence intensities have to be integrated over the layer thickness. The calculations are somewhat lengthy and are not presented here – an overview can be found *inter alia* in [1] or [2].

Finally for determination of the layers present in a given sample the measurement data, obtained by varying the incident angle of primary radiation across the critical angle of total reflection of the substrate and – in case of reflecting layers – the layer material, are evaluated by an iterative fitting procedure on the basis of modeling calculations. This procedure was developed and described by several authors [3,4].

To facilitate comparison of measurement data with the theoretical data described above and moreover conclusions on sample composition, the following demands have to be made on the instrumentation.

The angle between the incident beam and the reflector surface has to be very small to ensure external total reflection. The critical angle depends on the energy of the incident radiation and the material of the reflector. For primary X-rays of some 17 keV and a Si substrate it is in the range of 0.1° (1.74 mrad).

The primary beam should have a low height (with respect to the reflector surface) in the range of some 10 μm and a large width (about 10 mm) according to the detector crystal size. This can be realized by using an X-ray tube with a line focus and an aperture system restricting the beam in height. Other dimensions lead to unwanted scatter contributions.

For the investigation of thin layers angle dependent measurements have to be performed to obtain intensity profiles. Therefore it is necessary to be able to vary the angle of incidence between 0° and about 1° (17.4 mrad) depending on the used substrate. To get reasonable angular resolution of the intensity profiles the step-size of an angle scan should be below 0.01° (0.174 mrad). Further the adjusted angle has to be controlled with high accuracy (better than 0.005° (0.087 mrad)) to enable a reliable quantification of the intensity profiles.

It is necessary to use a monochromator because only a monochromatic incident beam produces the angle dependent intensity profiles that are distinctly determined by the layered samples. Therefore an intense spectral peak of the primary spectrum should be selected for excitation by a suitable monochromator – typically a multilayer monochromator acting as Bragg reflector. Spectral parts like other peaks than the selected one are unwanted because they would disturb the correlation between profile and layered sample.

2. Experimental

To avoid scattering of the primary X-rays in air and to minimize the absorption of low energetic fluorescence X-rays (e.g. Si, as Si emits 1.7 keV radiation and Si is used to normalize for quantification and dose determination) on their way to the detector, the whole setup is placed in a vacuum chamber with an overall size of $300 \times 300 \times 340 \text{ mm}^3$. The primary source is a 3 kW Mo-anode X-ray tube with a focal spot of $0.04 \times 12 \text{ mm}^2$ (long fine focus tube). In order to achieve low radiation background in the fluorescence spectra along

with suitable photon flux for thin-film analysis, the primary X-ray beam is monochromatized to 17.44 keV (Mo–K α) by means of a multilayer monochromator. To avoid unwanted effects due to totally reflected X-rays at the multilayer surface a 50 μm diaphragm is placed between multilayer and sample. The proper Bragg angle between incident radiation and multilayer surface is adjusted by positioning the X-ray tube using a stepper motor providing a linear translation of the tube versus a fixed slit. The movement is done until a maximum in the Mo–K α intensity is reached. The beam intensity after the multilayer is monitored by an ionization chamber. To process higher count rates a silicon drift detector (SDD, Vortex, from Radiant) with an active area of 50 mm^2 is used. The processing of high count rates is important as the Si signal increases drastically above the critical angle. The detector offers an energy resolution of 140 eV with 12 μs shaping time at 5.9 keV (Mn–K α) and a maximum processable count rate of 100 kcps. In order to perform all movements necessary for adjustment and measurement of the sample, the sample stage consists of 3 linear stages with a travel range of 25 mm each and one rotation stage allowing to perform angle scans in the range of $\pm 0.28 \text{ rad}$ with a minimum increment of 1.35 μrad . The stage can be tilted around the beam-axis to align the sample parallel to the beam. A sketch of the prototype spectrometer is shown in Fig. 1.

All GIXRF measurements were performed using the prototype for GIXRF analysis developed at Atominstitut, Vienna with the following parameters:

X-ray source: 3 kW Mo-tube LFF operated at 50 kV/40 mA and 50 kV/55 mA

Monochromator: multilayer from a commercial TXRF wafer analyzer (Atomika 8010 W)

Detector: Vortex 50 mm² SDD with provided Electronics Measurement (life) time: variable (20–120 seconds per point)

Angular resolution of each scan: variable (23–115 μrad)

Measurements were carried out in air and in vacuum (typical <1 mbar)

Several Arsenic implanted samples with implant dose from $1\text{E}14$ to $1\text{E}15$ and implant energy from 0.5 to 5 keV were measured. Aim of these measurements was to test the prototype and the acquisition

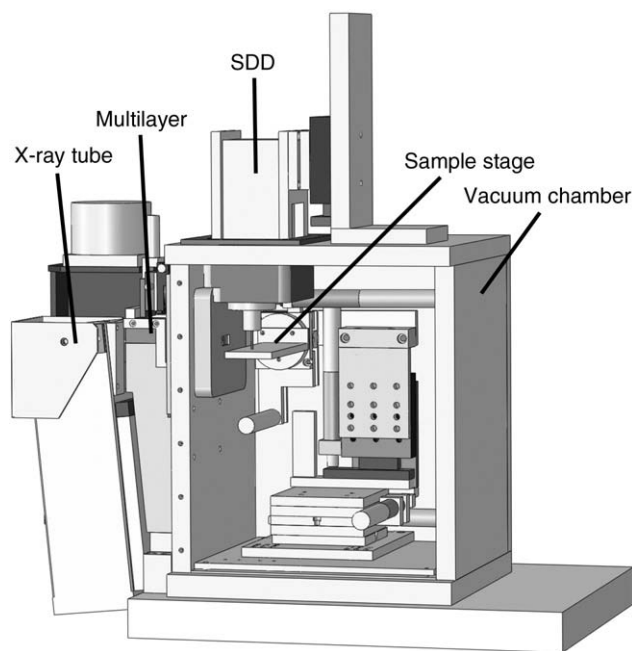


Fig. 1. Design of the recent version of the GIXRF spectrometer.

software and compare the results with the findings of Secondary Ion Mass Spectrometry (SIMS) and Instrumental Neutron Activation Analysis (INAA).

For further testing of the prototype and the acquisition software High-k (Hf) layer samples with layer thicknesses of 2 and 5 nm were measured.

For SIMS analysis As implanted samples were measured with a CAMECA Wf/SC-Ultra, magnetic sector secondary ion mass spectrometer, with a Cs^+ sputtering beam with impact energies of 500 keV ($\sim 45^\circ$ incidence angle) and collecting $^{28}\text{Si}^{75}\text{As}^-$ and $^{28}\text{Si}_2^-$ negative secondary ions. Sputtering time was converted to depth using a single constant sputtering rate as determined from the measurement of the final crater depth. $^{28}\text{Si}^{75}\text{As}^-$ secondary ion intensity was converted to As concentration using a relative sensitivity factor (RSF) determined from an As implant in Si of known dose. No corrections were applied to RSF in the initial transient width, surface SiO_2 layer and its interface with Si substrate.

For the determination of As in bulk samples, INAA is a method of choice [5]. For the current problem, INAA measurements have been carried out at the TRIGA Mark II reactor of the Atominstitut, Vienna University of Technology. Wafer pieces of about 3–4 cm^2 were weighed into polyethylene vials, sealed and irradiated for 1200 s using the pneumatic sample transfer system. The neutron flux density in this position is approximately $3 \cdot 10^{12} \text{ cm}^{-2} \text{ s}^{-1}$. After neutron irradiation, a cooling time of at least 60 min allowed the fast neutron activation products of silicon, ^{28}Al ($T_{1/2} = 2.2414 \text{ min}$) and ^{29}Al ($T_{1/2} = 6.56 \text{ min}$) to decay almost completely and allowed an undisturbed measurement of the thermal neutron activation product ^{76}As ($T_{1/2} = 1.0942 \text{ d}$). The measuring times were chosen independently for each sample, until the error due to counting statistics was $< 5\%$ rel. for the 559.1 keV peak of ^{76}As in each spectrum. All samples were measured in a fixed position at a distance of approximately 10 cm beside the detector so that the slightest possible changes in the geometry of the sample next to the detector could be neglected. The γ -spectrometry was performed with a 222 cm^3 HPGe-detector (1.78 keV resolution at the 1332 keV ^{60}Co peak; 48.2% relative efficiency), connected to a PC-based multi-channel analyzer with a preloaded filter and a Loss-Free Counting system. The area of the wafer pieces was calculated by derivation from the sample mass, Si density, and thickness. The total number of As atoms in the piece of wafer analyzed was determined by assuming that the sample with higher dose contained exactly $5 \cdot 10^{15} \text{ atoms/cm}^2$ (semi-quantitative analysis).

3. Results and discussion

Due to the vacuum capability of the spectrometer the calculation is simplified as no absorption in air has to be considered. The effect of the absorption for Si can be seen in Fig. 2.

Variable stepsize was used for the scans to gain a higher angular resolution at the critical angle of total reflection. Some mrad below and above the critical angle the angular increment was increased. The intensity differences in that region are getting smaller as the profile tends toward a constant value. For the sake of a reduced overall measuring time the angular resolution is decreased in these regions. Nevertheless they are important to measure, as these data are used for normalization. For all measurements the intensities recorded for the Si–K α line have been used for angle calibration. This is necessary as small differences between samples may result in a shift of the angle profile relative to the motor-position. Therefore the relation between motor position and absolute angle was recalibrated for each angular scan.

As the GIXRF measurement data represent the weighted integral of the depth profile up to a penetration depth of the X-rays, which depends on the incidence angle, and with the integral further modified by reflections on layers and standing wave patterns, the actual depth profile cannot be readily obtained. Based on an initial

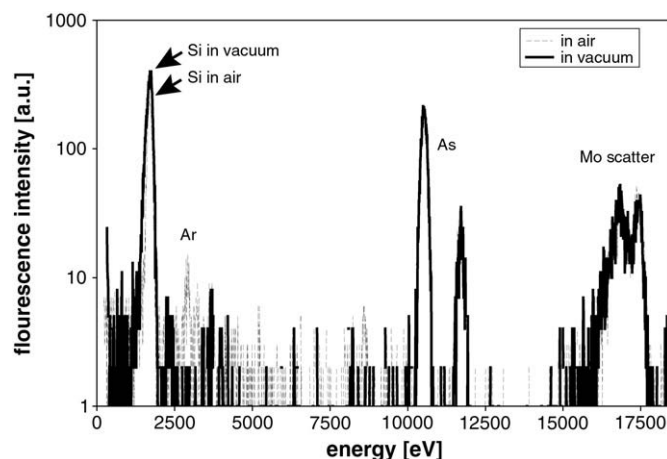


Fig. 2. The same sample measured in air and in vacuum. The rest of the measurement parameters (angle, height, inspected area) were kept constant. Mo tube at 50 kV/55 mA, 20 s livetime.

guess of the depth profile GIXRF data are calculated [3], compared to the measurement data and the guess modified until the calculation fits the measurement [4]. In the case of sufficiently smooth density changes (implants) or layers buried deeper in the substrate, the profile cannot be resolved unambiguously [6]. Still in such circumstances GIXRF can be used for the verification of the quality of the profile given by other techniques (e.g. SIMS [7]) or combined with other methods like ion beam sputtering [8] or etching [9].

3.1. Results of the implant samples

In the case of As implants a concentration profile obtained by SIMS was used as input and corrected. GIXRF and SIMS are used as complementary techniques, as GIXRF is very sensitive in the first few nanometers, where SIMS is not accurate enough [10], while deeper in the substrate the situation is reversed.

The Si (bulk/substrate) curve is fitted to have an evaluation of three instrumental parameters: (1) the offset in the angle, (2) the divergence of the beam and (3) a flux/geometry factor (represented by a scale factor on the curve). The total implanted dose can then be calculated according to [11] and [12].

Furthermore these parameters are used for processing and fitting of the Arsenic angular curve: The angle offset is used to correct the angular scale of the As intensity curve, the divergence value is used as initial estimate of the divergence in the As fit and the geometry factor is used as a scaling factor. In the calculation surface roughness has not been taken into account. In the fluorescence angular scan, a relevant roughness would be visible with an offset of the curve at small angles (higher fluorescence counts than expected at low angles).

The SIMS profile is assumed to be correct in the depth and can be given some degrees of freedom in the surface layer. The modifications of the SIMS profile can be parameterized, and the parameters can be determined with a best fit procedure. In particular three parameters can be considered for the “correction” of the SIMS profile: (1) The depth of the correction, (2) the sputtering rate (modification/scaling of the X-axis) and (3) a relative sensitivity factor (modification/scaling of the Y-axis).

An overview of the fitting procedure is shown in Fig. 3.

Figs. 4 and 5 show measured intensity profiles of Si and As respectively, and a comparison with calculated curves. The X-ray tube was operated at 50 kV/40 mA, acquisition time was 20 s livetime per point. The curves were calculated and modified for beam divergence using an algorithm developed in [7]. By means of the iterative fitting algorithm described above the parameters matching the measured data were determined. The beam divergence was taken into account

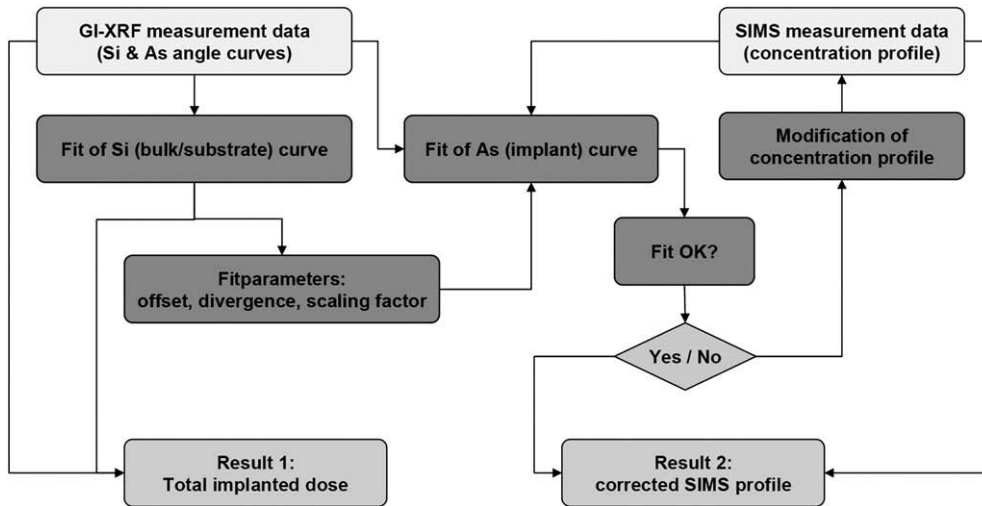


Fig. 3. Flowchart of the evaluation process for GIXRF measurements in combination with SIMS profiles.

by convoluting the theoretical data with a Gaussian function. Here, the FWHM value of the Gaussian function was varied until best agreement with the experimental data was reached. The final FWHM value determines the total divergence of the beam being the sum of angular and energy divergence. In the presented case (Fig. 4) a beam divergence of 0.3mrad was calculated.

The dose values measured by GIXRF are compared with the results obtained with SIMS (500 eV) and INAA in Fig. 6. The data of the GIXRF quantification shows good agreement with the nominal values and the other techniques (error <10% for all measured samples).

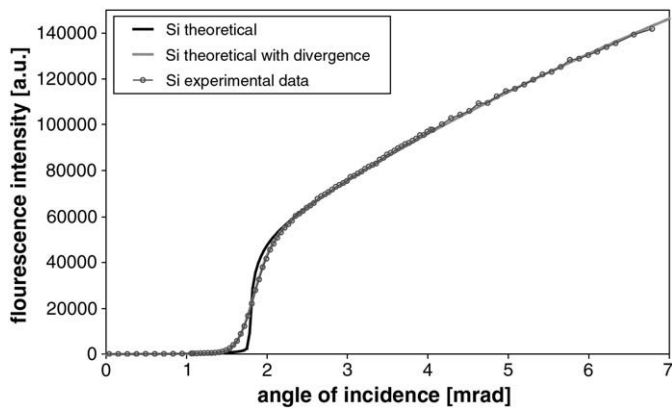


Fig. 4. Si fluorescence data from a Si-wafer with As-implant.

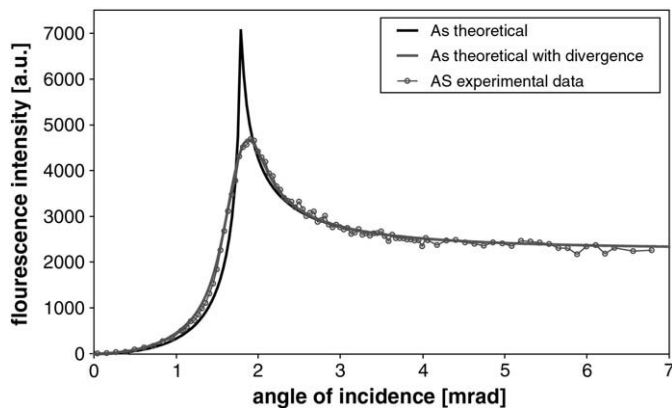


Fig. 5. As fluorescence data from a Si-wafer with As-implant.

Fig. 7 shows a SIMS profile, a TRIM simulated profile and the GIXRF profile resulting from the change of the SIMS profile by means of the developed fitting procedure for the GIXRF data. The Figure refers to a $1E15$ atoms/cm² implant of As atoms at 3 keV into Silicon. The GIXRF correction moves the SIMS profile into the depth. This is in agreement

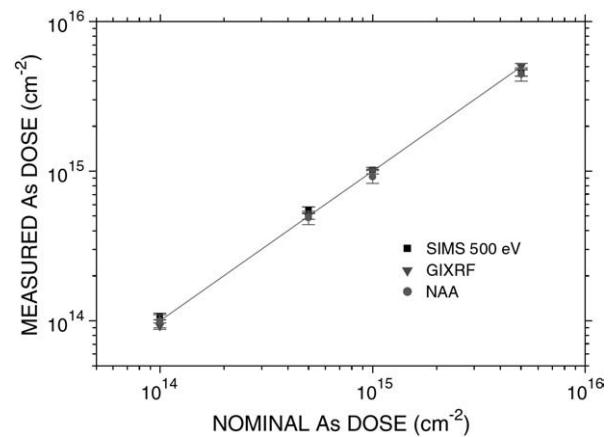


Fig. 6. Total retained fluence obtained with GIXRF, SIMS at 0.50 keV impact energy and INAA for the samples with constant implantation energy of 2 keV are displayed (adapted from [12]).

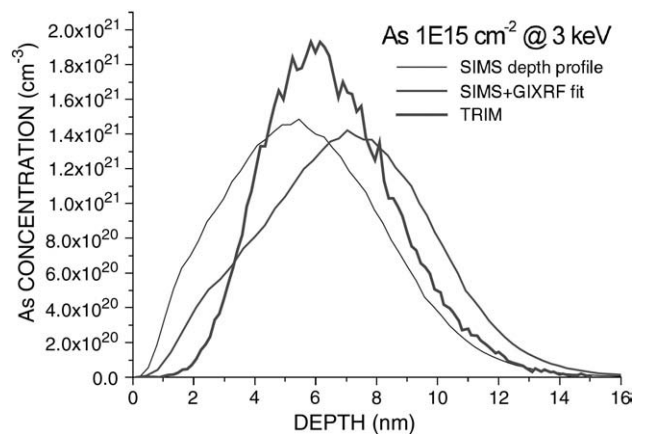


Fig. 7. SIMS profile, TRIM simulated profile and GIXRF profile resulting from the change of the SIMS profile by means of the developed fitting procedure for the GIXRF data.

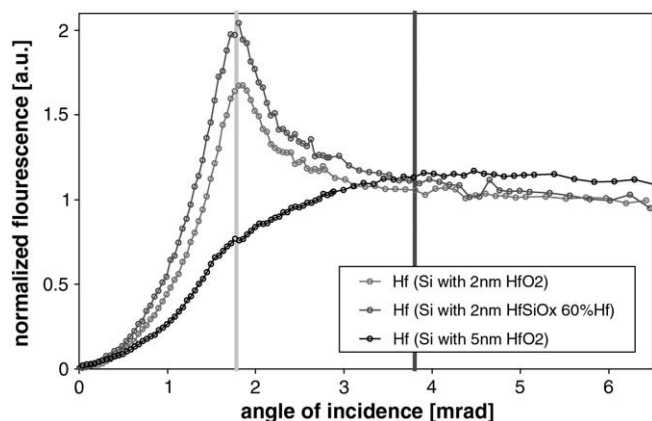


Fig. 8. Analysis results of Hf-oxide nanofilm samples. All profiles have been normalized to their intensities recorded for angles far below/beyond the critical angle of total reflection. The vertical lines indicate the critical angle of total reflection of Si (1.78mrad at 17.5 keV) and Hf (3.8mrad at 17.5 keV).

with the TRIM simulation. However the present correction seems to lead to a too deep junction depth. This is because GIXRF is very sensitive to the dopant concentration in the near surface region where SIMS is measuring a too high concentration of As atoms.

3.2. Results of the thin-film samples

The software package for fitting of thin-film samples is currently under development, nevertheless Hf-oxide film samples were measured and a qualitative comparison has been carried out, to evaluate the performance of the spectrometer.

To compare the shapes of the measured profiles, the curves have been normalized. Each profile has been normalized according to:

$$I = (\text{cps} - R_0) / (R_1 - R_0) \quad (3)$$

where cps are the measured peak intensities of the Hf-La line corrected for deadtime and normalized to counts per second, R_0 is the mean value of the first 5 data points of a scan and R_1 is the mean value of the last 5 data points of a scan. This normalization results in a profile where the region far below the critical angle is normalized to 0 whereas the angular region far beyond the critical angle is normalized to 1.

From the normalized results shown in Fig. 8 it is obvious that the shape of the 5 nm film profile is different from the ones for the 2 nm films. The maxima of the 2 nm profiles are located at the critical angle of Silicon (1.78 mrad for 17.5 keV excitation energy) whereas the 5 nm profile has no distinct maximum. This finding can be explained by reflections not only happening on the Si bulk layer, but also on the HfO_2 layer. All these findings are in good agreement with theory and data from literature [13].

4. Conclusions

Summarizing the presented results it could be shown that the prototype GIXRF spectrometer developed for implant and nanofilm analysis works sufficiently well.

Results of implant measurements were in good agreement with theoretical predictions and the used fitting algorithm worked properly. The dose quantification also showed good agreement with other techniques.

The measurements of thin-film samples delivered profile shapes in accordance with literature data and confirmed the applicability of instrumentation and data acquisition software for thin-film analysis. A software package for calculation and fitting of film samples is under development. The new version of the software takes into account roughness in the calculation of the E field penetrating but at the moment not for the fluorescence generated at low angles.

Acknowledgments

The authors would like to acknowledge support by the European Commission Research Infrastructure Action under the FP6 "Structuring the European Research Area" Programme through the Integrated Infrastructure Initiative ANNA (contract no. 026134-RII3).

References

- [1] R. Klockenkämper, Total Reflection X-Ray Fluorescence Analysis, Wiley-Interscience, New York, 1997.
- [2] D.K.G. de Boer, A.J.G. Leenaers, W.W. van den Hoogenhof, Glancing-incidence X-ray analysis of thin-layered materials: a review, X-Ray Spectrom. 24 (1995) 91–102.
- [3] D.K.G. de Boer, Glancing-incidence X-ray fluorescence of layered materials, Phys. Rev. B 44 (1991) 498–511.
- [4] U. Weisbrod, R. Gutschke, J. Knoth, H. Schwenke, Total reflection X-ray fluorescence spectrometry for quantitative surface and layer analysis, Appl. Phys. A: Mater. Sci. Process. 53 (1991) 449–456.
- [5] G. Steinhauser, W. Adlassnig, T. Lendl, M. Peroutka, M. Weidinger, I.K. Lichtscheidl, M. Bichler, Metalloid contaminated microhabitats and their biodiversity at a former antimony mining site in Schläining, Austria, Open Environ. Sci. 3 (2009) 26–41.
- [6] H. Schwenke, J. Knoth, Depth profiling in surfaces using total reflection X-ray fluorescence, Anal. Sci. 11 (1995) 533–537.
- [7] G. Pepponi, C. Strelti, P. Wobruschek, N. Zoeger, K. Luening, P. Pianetta, D. Giubertoni, M. Barozzi, M. Bersani, Nondestructive dose determination and depth profiling of arsenic ultrashallow junctions with total reflection X-ray fluorescence analysis compared to dynamic secondary ion mass spectrometry, Spectrochim. Acta Part B 59 (2004) 1243–1249.
- [8] H. Schwenke, J. Knoth, R. Gunther, G. Wiener, R. Bormann, Depth profiling using total reflection X-ray fluorescence spectrometry alone and in combination with ion beam sputtering, Spectrochim. Acta Part B 52 (1997) 795–803.
- [9] R. Klockenkämper, A. von Bohlen, A new method for depth-profiling of shallow layers in silicon wafers by repeated chemical etching and total-reflection X-ray fluorescence analysis, Spectrochim. Acta Part B 54 (1999) 1385–1392.
- [10] A. Parisini, V. Morandi, S. Solmi, P.G. Merli, D. Giubertoni, M. Bersani, J.A. Van den Berg, Quantitative determination of the dopant distribution in Si ultrashallow junctions by tilted sample annular dark field scanning transmission electron microscopy, Appl. Phys. Lett. 92 (2008) 261907.
- [11] P. Kregsamer, Fundamentals of total reflection X-ray fluorescence, Spectrochim. Acta Part B 46 (1991) 1332–1340.
- [12] G. Pepponi, D. Giubertoni, M. Bersani, F. Meirer, D. Ingerle, G. Steinhauser, C. Strelti, P. Hoenicke, B. Beckhoff, Grazing Incidence X-ray fluorescence and secondary ion mass spectrometry combined approach from characterization of ultra shallow arsenic distribution in silicon, International Workshop on INSIGHT in Semiconductor Device Fabrication, Metrology, and Modeling (INSIGHT-2009), Napa, California, USA, 2009, 26.04.2009 - 29.04.2009.
- [13] H. Schwenke, J. Knoth, U. Weisbrod, Current work on total reflection X-ray fluorescence spectrometry at the GKSS research centre, X-Ray Spectrom. 20 (1991) 277–281.